International Seminar on Student Research in Education, Science, and Technology
ISSN 3047-1532 | Volume 2 April 2025, pp. 659-671
https://www.issrestec.id/
http://journal.ummat.ac.id/index.php/issrestec
Universitas Muhammadiyah Mataram, Indonesia

Differential Pressure Fluctuations Analysis of Stratified to Annular Air-Water Transition Flow in Horizontal Pipe

Syaiful Tambah Putra Ahmad[1], Resky Gerhana Hidayatullah[1], Akhmad Afandi[2], Khasani[3], Deendarlianto[3]
[1]Department of Mechanical and Industrial Engineering, Universitas Gadjah Mada, Yogyakarta
[2]Department of Mechanical Engineering, Politeknik Negeri Banyuwangi
[3]Center for Energy Studies, Universitas Gadjah Mada, Sekip K-1, Kampus UGM, Yogyakarta
syaifultambahputraahmad@mail.ugm.ac.id, gerhanaresky@gmail.com, akhmad.afandi@poliwangi.ac.id, khasani@ugm.ac.id, deendarlianto@ugm.ac.id

Abstract: The transition of flow patterns from stratified to annular regimes in two-phase systems plays a critical role in determining flow stability, pressure drop, and the overall performance of pipeline operations. This study examined differential pressure fluctuations during the transition regime of air–water two-phase flow in a horizontal acrylic pipe with an internal diameter of 26 mm. Experiments were conducted at 12 flow conditions, with superficial gas velocities (J_G) ranging from 8 to 14 m/s and liquid velocities (J_L) from 0.08 to 0.2 m/s. Differential pressure data were collected in time series and analyzed using the Probability Density Function (PDF) and Power Spectral Density (PSD). The results indicated that increasing JG and JL enhanced interfacial interactions, promoted disturbance waves, and initiated entrainment, leading to the formation of annular flow. PDF analysis showed a shift from narrow peaks in stratified flow to wider, multi-modal distributions in the transition regime, signifying pressure instability. Correspondingly, PSD analysis revealed a rise in dominant frequency and spectral energy as the flow became more dynamic. These findings demonstrated that time series-based PDF and PSD analysis could effectively capture the evolving characteristics of flow regime transitions and serve as diagnostic tools for understanding two-phase flow behaviour.

Keywords: Two-Phase Flow, Flow Pattern Transition, Pressure Gradient, Annular Flow, Stratified Flow.

Article History:
Received: 01-04-2025
Online : 05-05-2025

A. INTRODUCTION

One of the critical aspects in the study of two-phase flow is the transition between flow patterns, particularly from stratified to annular flow. Understanding this transition process was essential, as it was directly related to interfacial stability, pressure variation, and dynamic fluid behaviour. In the stratified flow regime, the liquid and gas phases are clearly separated in a horizontal pipe, where the liquid phase occupies the bottom while the gas phase flows in the upper region. As the superficial velocities of gas (J_G) and liquid (J_L) increased beyond a certain threshold, a liquid film began to form along the pipe wall due to the influence of various forces occurring during the transition. These forces included disturbance waves (Zhao et al., 2013), secondary flows Westende et al. (2007), wave spreading (Jayanti et al., 1990), entrainment and deposition (Patruno et al., 2010), and wave pumping mechanisms (Höhne et al., 2015). When the annular flow regime is fully established, the liquid phase resides as a thin layer on the pipe walls, moving at relatively low velocities, while the gas phase dominates the central core, moving at much higher velocities. In pipeline industries, maintaining annular flow is highly important due to its significant influence on heat transfer efficiency and corrosion protection (Tso & Sugawara, 1993).

Previous studies have explored the flow transition phenomenon from various perspectives. Cherdantsev et al. (2022) investigated through visualization that secondary flow acted as the primary mechanism for the formation of the thin liquid layer along the pipe wall during annular flow conditions (Cherdantsev et al., 2022). The stability of this film was also influenced by gravitational forces, which led to an asymmetric distribution of the liquid film (Baik & Hanratty, 2003). Rodrigues et al. (2018) proposed a modelling approach that considered the effect of the liquid film on pressure gradient calculations (Rodrigues et al., 2018). On the other hand, Vieira et al. (2014, 2013) investigated stratified and annular flows using statistical time-series analysis of void fraction data through Probability Density Function (PDF) and cross-correlation methods. However, they did not explicitly address the transition regime (Vieira et al., 2014, 2013). Shmueli and Unander. (2015) observed that the pressure gradient increased systematically with the rise in J_G (Shmueli et al., 2015).

Wang et al. (2024) investigated stratified and annular flows under high-pressure conditions and found that transition flow could occur even at relatively low J_L (Wang et al., 2024). They also observed that increased pressure made the interface more unstable, which was attributed to the higher gas-phase density and enhanced momentum transfer between phases. Meanwhile, Khan et al. (2023) emphasized that pressure fluctuations could be a reliable indicator for identifying flow patterns, as each regime exhibited distinct dominant frequencies and unique characteristics in their PDF profiles (Khan et al., 2023).

Based on previous studies, the transition from stratified to annular flow has received significant attention due to its critical importance in the design and operation of pipeline systems, particularly in multiphase flow applications. However, few investigations have focused explicitly on time-dependent pressure fluctuations during this transition phase. Understanding the transition phenomenon through a time-dependent pressure analysis could offer valuable insights into system stability and flow pattern prediction. Addressing this gap, the present study focused on observing differential pressure fluctuations during the transition from stratified to annular flow. This study conducted a comprehensive analysis of pressure behaviour during the flow transition by applying signal processing methods, including the PDF and Power Spectral Density (PSD), to characterize the pressure signal profiles. This time-dependent analysis was expected to enhance understanding of flow transition phenomena and contribute to a more comprehensive interpretation of two-phase flow dynamics.

B. METHOD

1. Experimental Facility

The test system consisted of three main components: air circulation, water circulation, and the test section with a data acquisition system. A schematic diagram of the experimental configuration is shown in Figure 1. A compressor supplied the air flow with a pressure of 8 kg/cm^2 and a capacity of 275 litres. The airflow was regulated using a regulator and measured with a flowmeter. The water circulation involved two 50-litre tanks and a pump with a flow rate of 100 LPM. The water was controlled using a valve and measured with a flowmeter. The air and water were mixed in a mixer and channelled through a transparent acrylic pipe with a diameter of 26 mm and a length of 10 meters, with lighting provided for flow visualization. Differential pressure measurements were obtained using a Differential Pressure Transducer (DPT), which was integrated with a data acquisition (DAQ) system to facilitate real-time time-series recording for analyzing flow dynamics.

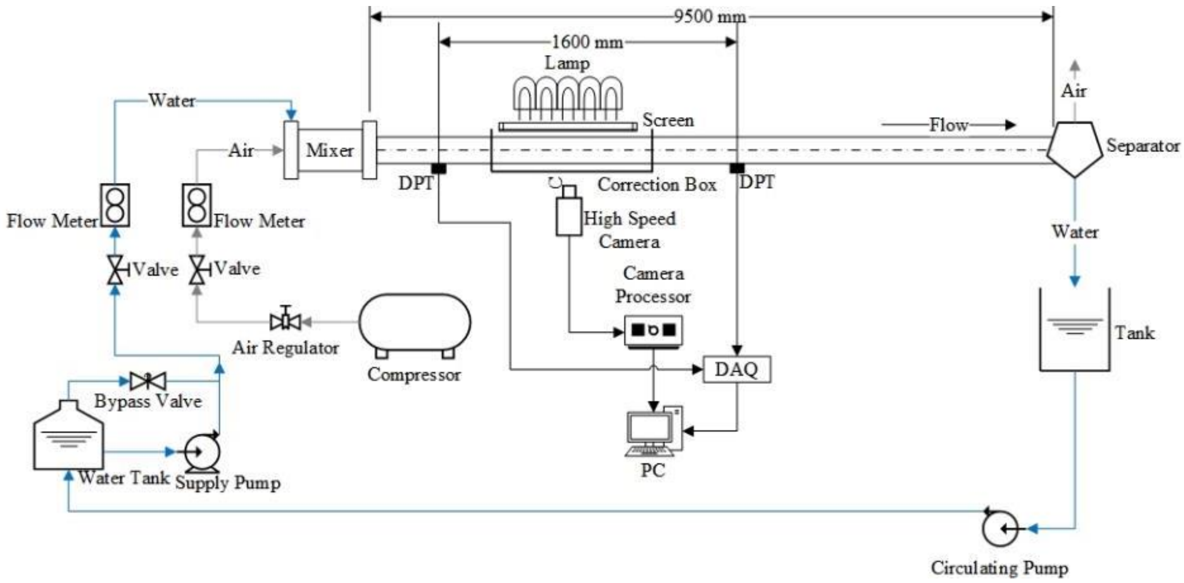

Figure 1. Experimental Apparatus

2. Research Variable

This study employed three variables: dependent, independent, and controlled, which were determined based on literature reviews and previous research.

a. Dependent Variable

The dependent variable in this study was the pressure fluctuations observed specifically during the stratified-to-annular flow transition. The differential pressure was recorded as a time-dependent signal to capture the dynamic evolution of the flow structure.

b. Independent Variable

The independent variables in this study were J_G and J_L. The J_G values ranged from 8 to 14 m/s, while J_L varied at 0.08, 0.1, and 0.2 m/s. As outlined in the test matrix presented in Figure 2, 12 experimental combinations were conducted. These combinations aimed to comprehensively investigate the effect of velocity variation on pressure characteristics during the flow pattern transition.

c. Controlled Variable

Several variables were strictly controlled throughout the experiment to ensure the validity of the results. The working fluids used were air and water, with their physical properties referred to Yaws (2015), as presented in Table 1 (Yaws, 2015). The test section consisted of a pipe with an internal diameter of 26 mm and a length of 9.5 m. The internal pressure of the pipe was maintained at a constant 0.7 MPa using a regulator, while ambient temperature and pressure were kept at standard laboratory conditions

(25°C, 1 atm). The pipe's inner surface was carefully cleaned and kept smooth prior to each experiment to minimize the influence of surface roughness on the measurement results.

Table 1. Fluid Properties

Properties	Symbols	Water (H_2O)	Gas (Air)	Units
Density	ρ	1012.111	1.184	kg/m³
Dynamic Viscosity	μ	8.82E-04	1.83E-05	Pa.s
Kinematic Viscosity	v	8.71E-07	1.54E-05	m²/s
Surface Tension	σ	0.073	-	N/m
Heat Capacity	Cp	76.390	29.148	J/mol K
Thermal Conductivity	k	0.608	0.026	W/m K

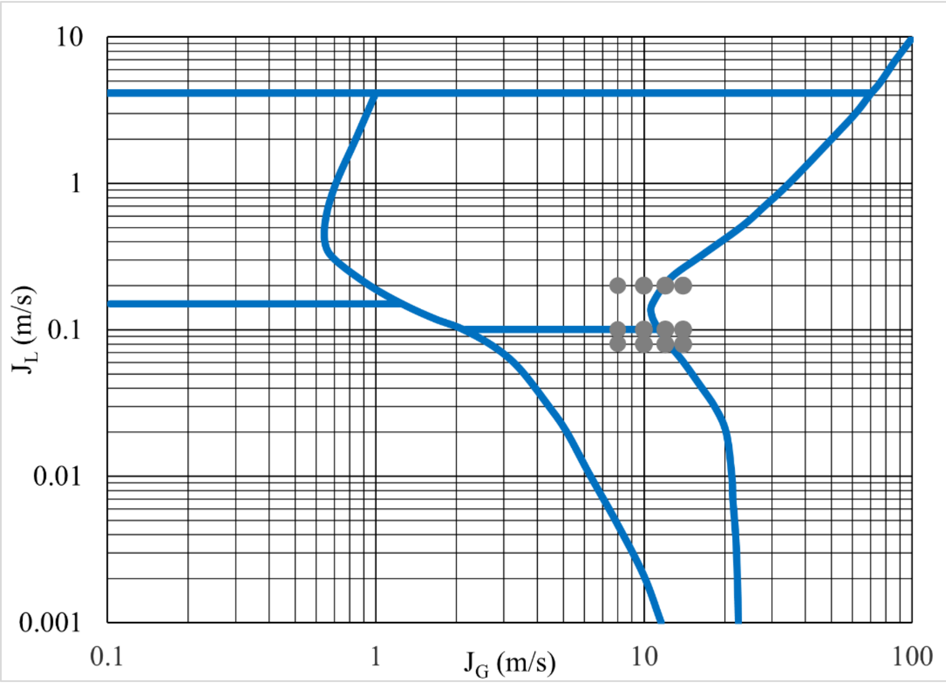

Figure 2. Research Variables

3. Experimental Methods

a. Probability Density Function

In this study, the PDF was widely employed to analyze two-phase flow, as demonstrated in previous works by Abdulkareem et al. (2021) for flow identification and Yang et al. (2023) for flow pattern analysis using conductivity measurements (Abdulkareem et al., 2021; Yang et al., 2023). The PDF was utilized to investigate the distribution of differential pressure fluctuations during the transition from stratified to annular flow. The computation entailed segmenting the pressure data into discrete intervals (bins), quantifying the data points in each bin, and normalizing these counts by the total number of observations and the bin width to derive the probability density function. The formulation is expressed as follows:

$$f(x) = \frac{n_i}{N \cdot \Delta x} \quad (1)$$

Where:

- $f(x)$: PDF value at interval x
- n_i : number of data points within i-th interval
- N : total number of data points
- Δx : interval width (bin width)

The pressure data from the differential sensor were converted into time-series form and processed to compute the PDF values for each experimental variable. The resulting PDF distributions enabled the identification of pressure characteristics, such as narrow distributions under stable flow conditions and broader or asymmetric distributions during flow transitions. This analysis provided a foundation for evaluating the system's dynamic behaviour across different combinations of J_G, J_L, and identifying unique features of pressure distribution associated with flow regime changes. The PDF analysis also functioned as a preliminary step before performing further spectral evaluation using PSD.

b. Power Spectral Density

The Power Spectral Density (PSD) analysis in this study was employed to evaluate the frequency components of differential pressure fluctuations during the evolution of flow pattern. Nnabuife et al. (2021) demonstrated that PSD effectively reveals significant pressure fluctuations and interfacial interactions, thereby assisting in identifying flow patterns and transitions (Nnabuife et al., 2021). Similarly, Catrawedarma et al. (2021) employed PSD analysis to examine gas–liquid flow within an airlift bubble generator, showing that variations in the PSD curve shape correspond to flow regime transitions and visually indicate flow stability or instability (Catrawedarma et al., 2021).

Building upon these findings, this study obtained pressure data in time-series form using a DAQ system connected to a DPT. The signals recorded in the time domain were subsequently converted into the frequency domain through the application of the Fast Fourier Transform (FFT) technique. This transformation generated a power spectrum illustrating how the signal's energy is distributed across various frequency components. In this approach, the time-series signals were divided into segments, each with a duration defined as:

$$x_i(n) = x(n + iN_s) \quad (2)$$

Where $i = 1,2,3, ..., L$ represented the segment index, and $n = 1,2,3, ..., N_s$ denoted the data index within each segment. This segmentation enabled local analysis of the signal to improve the reliability of the spectral transformation results, allowing for more detailed observation of oscillation patterns across different frequency ranges. The power spectrum for each segment was calculated using the following equation:

$$P_{xx}^{i}(f) = \frac{1}{N_s U} \left| \sum_{N=1}^{N_s} x_i(n) w(n) \exp\left(-j2\pi f n\right) \right|^2 \quad (3)$$

Where $w(n)$ denoted the window function, and U was the normalization factor, defined as:

$$U = \frac{1}{N_s} \sum_{N=1}^{N_s} w^2(n) \tag{4}$$

Finally, the average power spectral density across all segments was formulated as:

$$P_{xx}(f) = \frac{1}{L} \sum_{i=1}^{L} P_{xx}^{i}(f) \tag{5}$$

These equations formed the basis for calculating , which evaluates the distribution of signal power across frequency components within the two-phase flow system (Catrawedarma et al., 2021).

C. RESULTS AND DISCUSSION

1. Visual Observation of Two Phase Flow

In this experimental study conducted within a horizontal pipe, variations in J_G and J_L led to observable changes in flow patterns, providing valuable insights into interfacial dynamics and flow transition mechanisms. In this study, visual observation was employed to verify the progression of flow patterns transition from stratified to annular flow, driven by physical forces acting within the system. Under the initial condition of JG = 8 m/s and JL = 0.08 m/s (Figure 3), the flow exhibited characteristics of a stable stratified regime. The liquid phase flowed along the bottom of the pipe while the gas moved along the top, forming a flat and distinct interface. In this configuration, gravitational forces played a dominant role in maintaining the separation between phases, with the liquid settling at the bottom and the gas occupying the top section of the pipe.

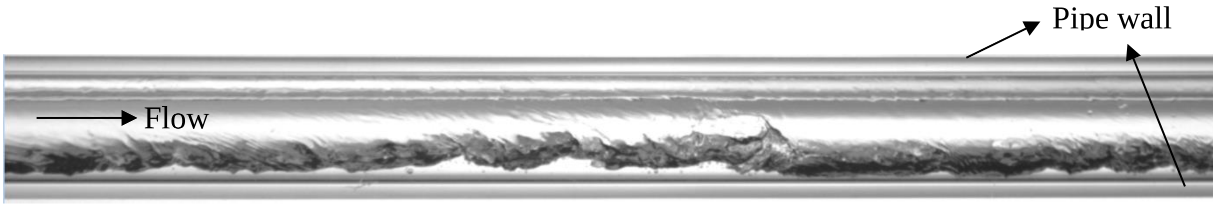

Figure 3. Stratified flow (J_G 8 m/s and J_L 0.08 m/s)

As J_G was increased to 10 m/s while J_L remained constant at 0.08 m/s (Figure 4), the flow entered a transitional phase, marked by the emergence of interfacial waves along the liquid–gas surface. These waves indicated an onset of instability at the interface between the two phases. The increase in gas velocity induced turbulent forces that disrupted the stability of the phase separation and generated propagating waves along the pipe. In Figure 5, the transitional flow pattern became more pronounced. The interfacial waves grew more irregular, with portions of the liquid detaching from the film and becoming entrained by the gas phase. This behaviour reflected the growing dominance of inertial forces, resulting in the liquid phase no longer being completely confined to the bottom of the pipe. Entrainment occurred as the gas began to carry the liquid, indicating an increasingly intense interaction between the two phases. A liquid film appeared along the pipe wall, although it remained unstable.

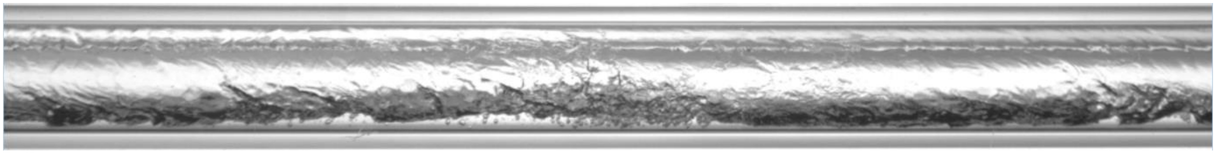

Figure 4. Transition flow (J_G 10 m/s and J_L 0.08 m/s)

Figure 5. Transition flow (J_G 10 m/s and J_L 0.1 m/s)

At the highest test condition, with J_G = 14 m/s and J_L = 0.2 m/s (Figure 6), the flow had fully transitioned into the annular flow regime. The liquid phase formed a thin, continuous film along the pipe wall, while the gas phase flowed rapidly through the core region, forming a central gas core. Under this condition, the increased shear forces between the gas and liquid phases triggered strong turbulence within the system, generating larger disturbance waves and more intense interfacial interactions. The entrainment phenomenon became more prominent, where liquid droplets detached from the film and were carried by the high-velocity gas, resulting in an unstable liquid distribution along the pipe. The high gas inertia further destabilized the liquid film, developing highly dynamic and complex flow structures. Visual observations confirmed that the interplay of gravitational, frictional, inertial, and turbulent forces governed the transition flow.

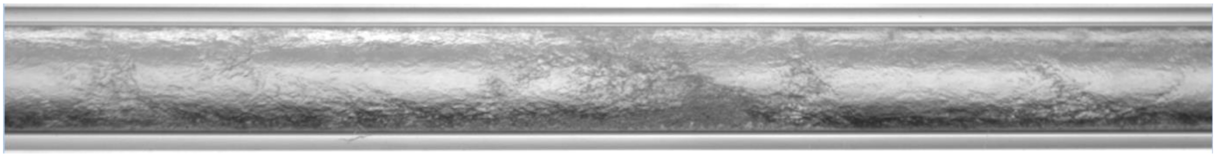

Figure 6. Annular flow (J_G 14 m/s and J_L 0.2 m/s)

2. Pressure Gradient Fluctuation

Differential pressure fluctuations in this study significantly increased with the rise in J_G and liquid J_L. As shown in Figure 7, the time-series data of $\Delta P/L$ revealed that, at a low liquid velocity (J_L = 0.08 m/s), the amplitude of pressure fluctuations was relatively small, indicating weak interfacial interactions and a flow regime that remained largely stratified. However, when J_G exceeded 10 m/s, disturbance waves emerged, resulting in a broader variation of $\Delta P/L$. An increase in J_L to 0.1 m/s further amplified this effect as shear forces and turbulence became more dominant, widening the pressure oscillation range and signaling the onset of a transitional flow regime. At the highest tested J_L value (0.2 m/s), the fluctuation amplitude peaked particularly at J_G = 14 m/s, indicating the establishment of annular flow. Under this condition, the high gas velocity compelled the liquid phase to form a wall-bound film, enhancing entrainment and inertial forces. This subsequently led to a surge in differential pressure. The observed pattern confirmed that simultaneous increases in J_G and J_L significantly intensified interfacial interactions, friction, and turbulence. This drove the flow from a stable stratified state toward a dynamic annular regime characterized by more significant and irregular pressure fluctuations.

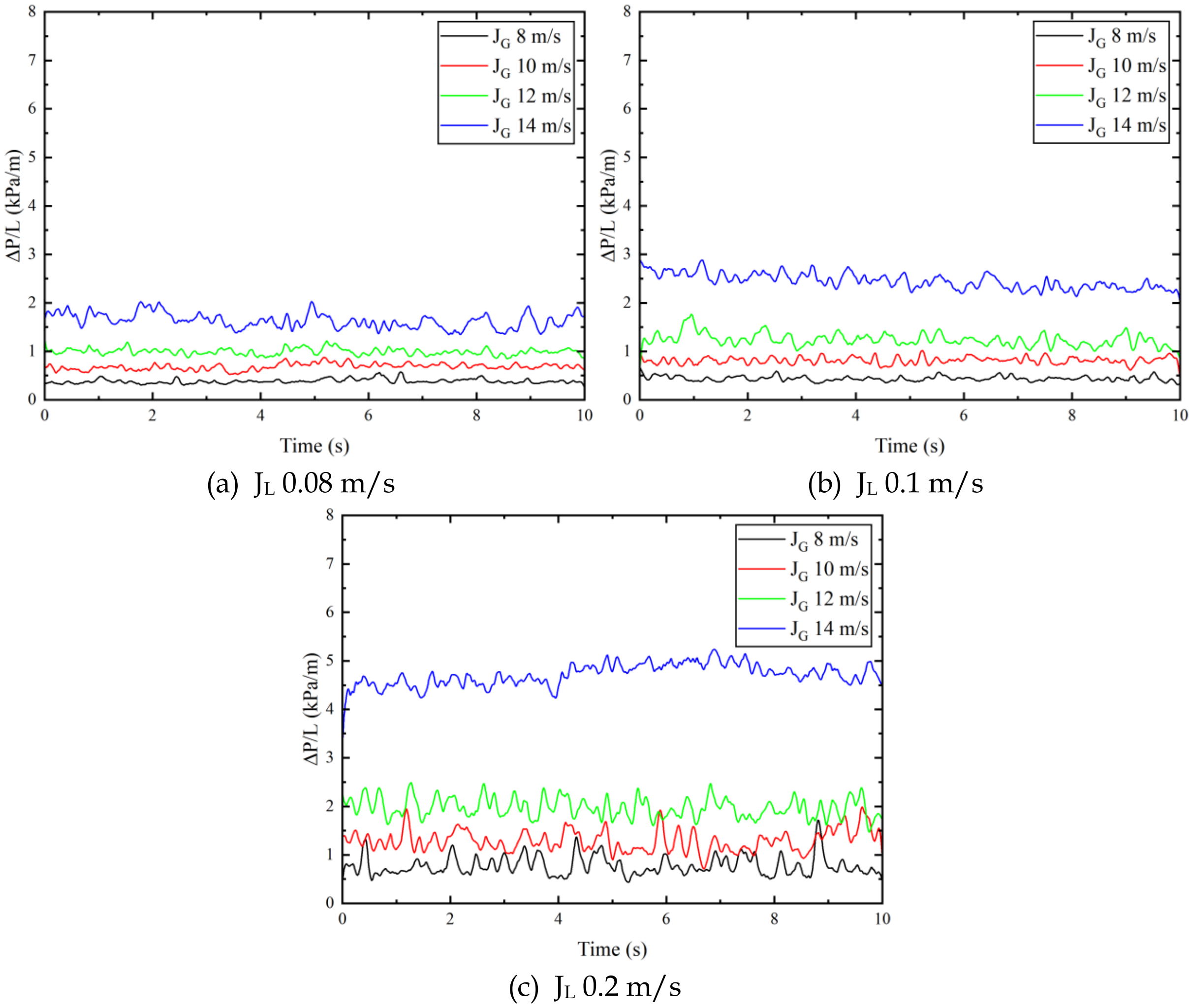

Figure 7. Differential Pressure Fluctuation at Various J_L value.

3. The Probability Density Function (PDF)

The analysis of the Probability Density Function (PDF) shown in Figure 8 offers detailed insights into the evolution of pressure gradient distribution as J_G and J_L increase. At J_L = 0.08 m/s, the PDF is concentrated around a narrow range of lower ΔP/L values with a sharp peak, indicating minor pressure fluctuations and relatively stable flow conditions—characteristic of a stratified flow regime where the liquid and gas phases remain distinctly separated. As J_G increases, the PDF peak shifts toward higher ΔP/L values, reflecting the growing influence of shear stress and turbulence, intensifying interfacial disturbances.

This phenomenon becomes more evident at J_L = 0.1 m/s (Figure 8 (b)), where the PDF broadens, suggesting enhanced shear interactions between the phases and the onset of transitional behaviour. The system begins to deviate from stratified stability toward a more dynamic regime. At J_L = 0.2 m/s, the distribution shifts to the right with a broarder and higher peak, particularly at J_G = 14 m/s. This trend reflects the establishment of annular flow, characterized by forming a thin liquid film along the pipe wall and the passage of high-velocity gas through the core. The intensified interfacial interaction, driven by greater inertial and turbulent forces, results in more significant and irregular pressure fluctuations. These shifts in PDF distribution clearly illustrate the increasing dominance of inertial and turbulent effects, consistent with the rising pressure fluctuation amplitudes discussed in the previous section.

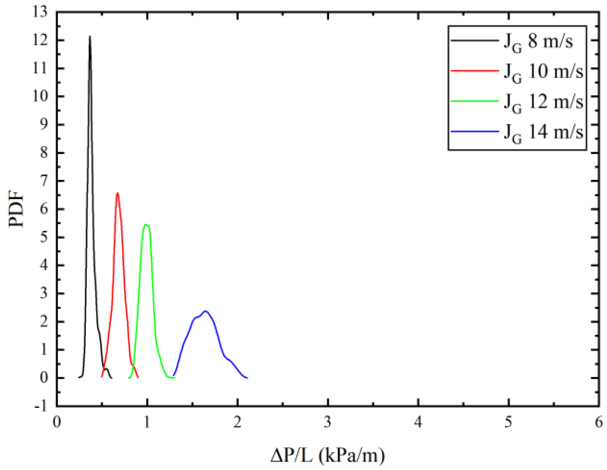

(a) J_L 0.08 m/s

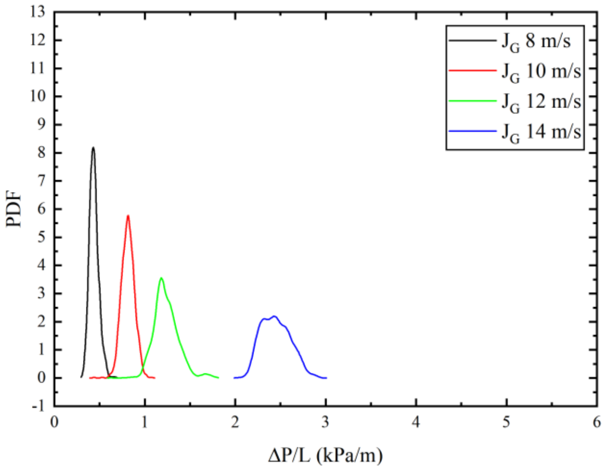

(b) J_L 0.1 m/s

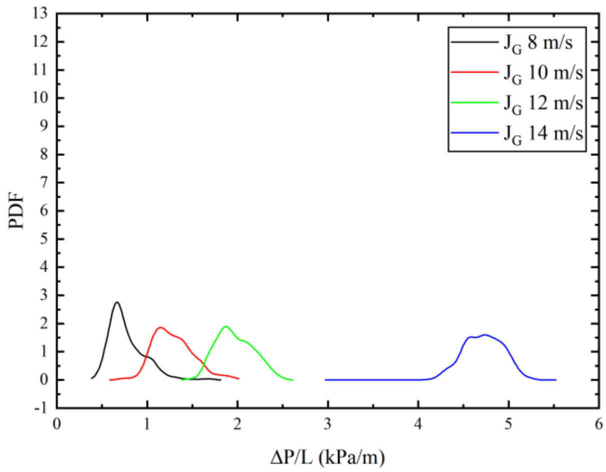

(c) J_L 0.2 m/s

Figure 8. PDF at Various J_L value

4. The Power Spectral Density (PSD)

The dynamic characteristics of two-phase flow can be analyzed through the PSD, as illustrated in Figures 9 and 10. In Figure 9, both the dominant frequency (fmax) and magnitude provide insight into the intensity of pressure oscillations within the system. Under stratified flow conditions (Figure 9 (a)), fmax is relatively low (0.586 Hz), and the corresponding magnitude is also small. This reflects a stable flow regime, where minimal interfacial interaction occurs as the liquid and gas phases flow separately horizontally. Consequently, pressure fluctuations remain confined to low frequencies and exhibit low energy. As the flow enters the transitional regime (Figures 9 (b) and 9 (c)), significant spectral changes emerge. The dominant frequency varies (0.195 Hz and 2.148 Hz) depending on the strength of interfacial disturbances induced by increasing J_G and liquid J_L. These conditions lead to more intense wave generation and turbulence, shifting the energy concentration to higher frequencies. The corresponding rise in PSD magnitude indicates enhanced energy input into the system due to the more vigorous phase interactions. In the annular flow regime (Figure 9 (d)), the dominant frequency increases to 1.367 Hz, with the highest magnitude among all flow conditions. This can be attributed to the predominance of inertial and shear forces, which promote the formation of a liquid film along the pipe wall and droplet entrainment by high-speed gas in the core. These effects lead to high-frequency pressure oscillations and greater spectral energy, signifying a higher degree of flow instability typically associated with the annular regime.

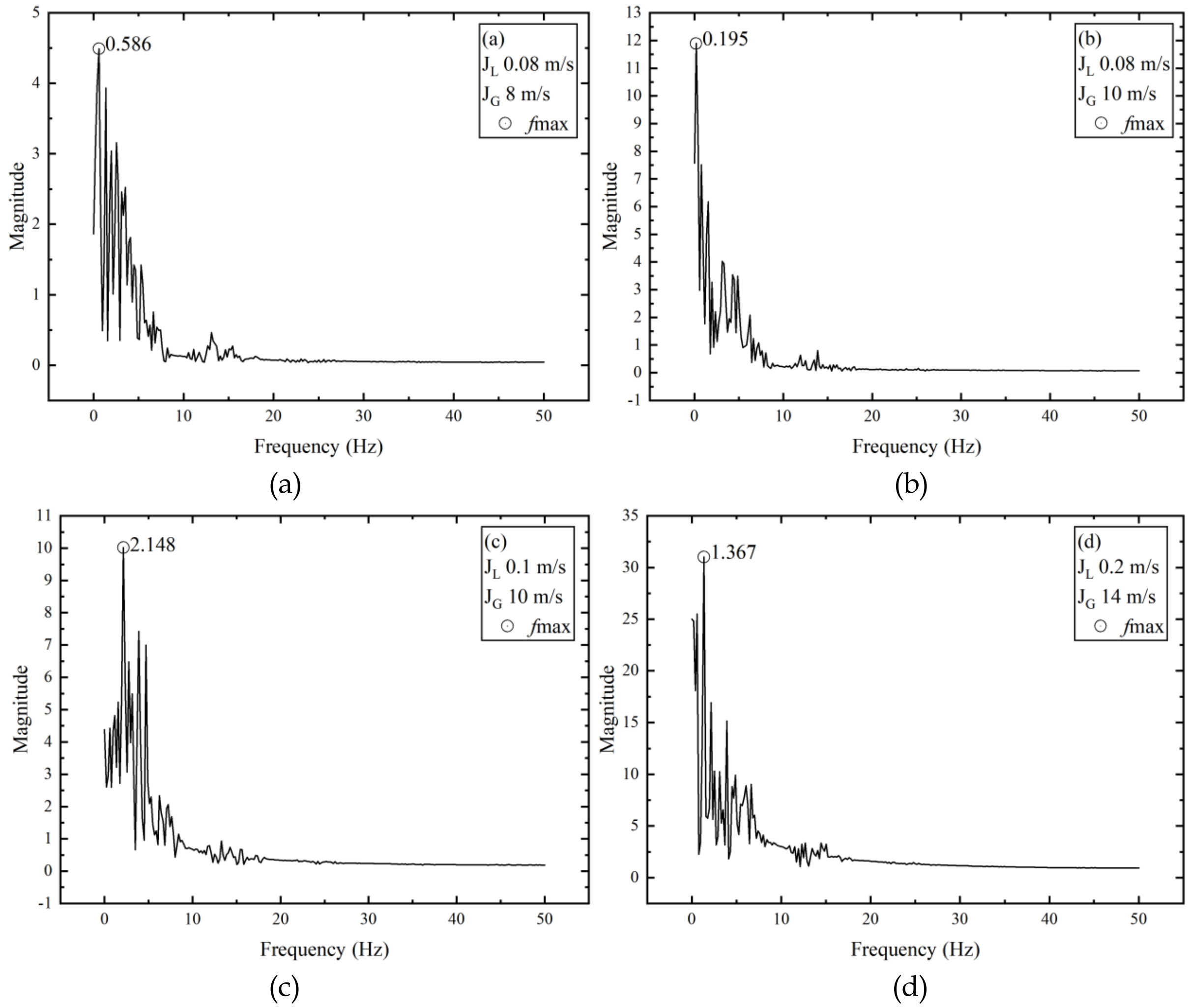

Figure 9. PSD at Various J_L value, (a) Stratified, (b – c) Transition, and (d) Annular Flow

Figure 10 illustrates the correlation between the dominant frequency (Figure 10 (a)) and the maximum PSD (Figure 10 (b)) under various combinations of J_G and J_L. In Figure 10 (a), the dominant frequency shows an increasing trend with rising values of J_G and J_L, indicating stronger interfacial interactions between the gas and liquid phases. As J_L rises from 0.08 m/s to 0.1 m/s, the dominant frequency increases, indicating more pronounced disturbance waves and the initiation of transitional flow behaviour. However, when J_L reaches 0.2 m/s, the dominant frequency remains relatively stable within the mid-frequency range. This indicates forming a thicker liquid film along the pipe wall, which acts as a damping layer against high-frequency perturbations.

In Figure 10 (b), the PSD maximum rises significantly with increasing J_G and J_L, indicating an overall increase in the energy of pressure fluctuations. This observation is consistent with the evolution flow pattern from stratified to annular flow, where shear stress and interfacial friction intensify due to higher flow rates in both phases. As a result, the amplitude of pressure signals becomes larger. Gas-liquid interaction strongly influences both the dominant frequency and the magnitude of spectral energy. The increased activity of disturbance waves and droplet entrainment at higher flow rates accelerates the transition to annular regime, which is characterized by more significant, more complex pressure fluctuations and a broader energy spectrum.

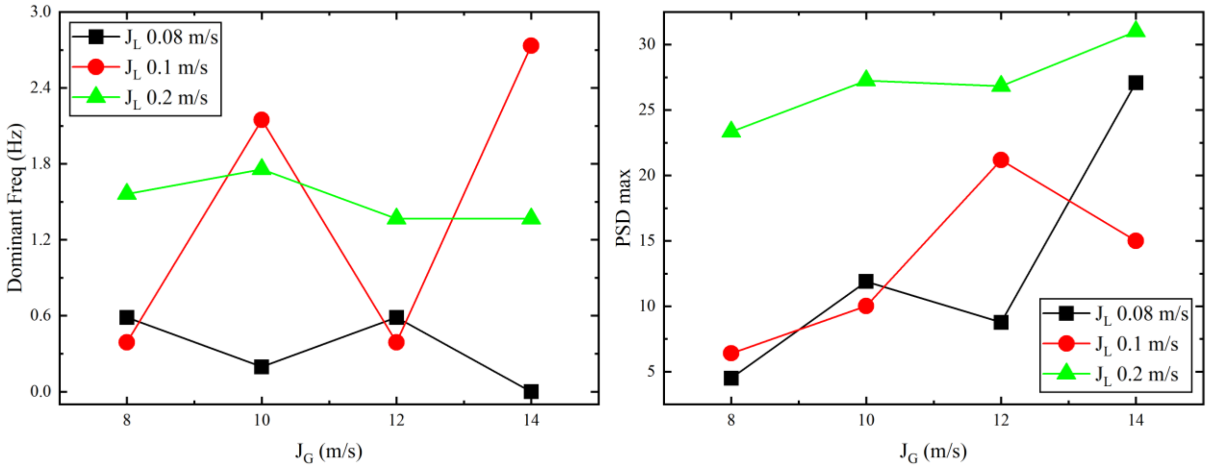

(a) (b)

Figure 10. PSD characteristics under various flow condition, (a) Dominant Frequency, and (b) PSD max

D. CONCLUSIONS AND SUGGESTIONS

This study thoroughly examined the dynamics of the two-phase flow transition from stratified flow to annular flow in a horizontal pipe, with a focus on differential pressure fluctuations as the primary indicator of flow pattern changes. Based on visual observation, time-series pressure analysis, PDF distribution, and PSD spectrum, it was found that the increase in JG and liquid JL velocities significantly influenced interfacial interactions, generated disturbance waves, and accelerated the entrainment process, ultimately shifting the system toward a more dynamic and unstable annular flow regime.

Pressure fluctuations increased sharply with rising J_G and J_L, as indicated by the widening of the PDF distribution and the shift of its peak value, suggesting system instability during the transition phase. Simultaneously, the PSD analysis showed a progressive increase in dominant frequency (fmax) and maximum PSD value, reflecting higher turbulence energy and pressure oscillation intensity characteristic of annular flow. Each flow regime exhibited distinct spectral characteristics that could be identified through frequency-domain analysis. Therefore, this study demonstrated that a time-dependent pressure fluctuation approach using PDF and PSD analyses was practical in quantitatively and systematically characterizing two-phase flow transitions and holds potential as a reference for evaluating the performance of multiphase pipeline systems.

ACKNOWLEDGMENTS
The authors would like to express their sincere gratitude to Direktorat Riset, Teknologi, dan Pengabdian kepada Masyarakat (DRTPM), Direktur Jenderal Pendidikan Tinggi, Riset, dan Teknologi (Diktiristek), Ministry of Higher Education, Science, and Technology of the Republic of Indonesia, for the financial support provided through the PMDSU Batch VII scheme.

REFERENCES
Abdulkareem, L. A., Musa, V. A., Mahmood, R. A., & Hasso, E. A. (2021). Experimental Investigation of Two-Phase Flow Patterns in a Vertical to Horizontal Bend Pipe Using Wire-Mesh Sensor. *Revista de Chimie*, *71*(12), 18–33. https://doi.org/10.37358/rc.20.12.8383

Baik, S., & Hanratty, T. J. (2003). Concentration profiles of droplets and predicion of the transition from stratified to annular flow in horizontal pipes. *International Journal of Multiphase Flow*, *29*(2), 329–338. https://doi.org/10.1016/S0301-9322(02)00126-X

Catrawedarma, I. G. N. B., Deendarlianto, & Indarto. (2021). Statistical Characterization of Flow Structure of Air–water Two-phase Flow in Airlift Pump–Bubble Generator System. *International Journal of Multiphase Flow*, *138*. https://doi.org/10.1016/j.ijmultiphaseflow.2021.103596

Cherdantsev, A. V., Zdornikov, S. A., Cherdantsev, M. V., Isaenkov, S. V., & Markovich, D. M. (2022). Stratified-to-annular gas-liquid flow patterns transition in a horizontal pipe. *Experimental Thermal and Fluid Science*, *132*. https://doi.org/10.1016/j.expthermflusci.2021.110552

Höhne, T., Geissler, T., Bieberle, A., & Hampel, U. (2015). Numerical modeling of a horizontal annular flow experiment using a droplet entrainment model. *Annals of Nuclear Energy*, *77*, 351–360. https://doi.org/10.1016/j.anucene.2014.11.041

Jayanti, S., Hewitt, G. F., & White, S. P. (1990). Time-dependent behaviour of the liquid film in horizontal annular flow. *International Journal of Multiphase Flow*, *16*(6), 1097–1116. https://doi.org/10.1016/0301-9322(90)90108-U

Khan, U., Pao, W., & Sallih, N. (2023). Numerical Gas–Liquid Two-Phase Flow Regime Identification in a Horizontal Pipe Using Dynamic Pressure Data. *Applied Sciences (Switzerland)*, *13*(2). https://doi.org/10.3390/app13021225

Nnabuife, S. G., Sharma, P., Iyore Aburime, E., Lokidor, P. L., & Bello, A. (2021). Development of gas-liquid slug flow measurement using continuous-wave doppler ultrasound and bandpass power spectral density. *ChemEngineering*, *5*(1), 1–14. https://doi.org/10.3390/chemengineering5010002

Patruno, L. E., Marchioro Ystad, P. A., Jenssen, C. B., Marchetti, J. M., Dorao, C. A., Svendsen, H. F., & Jakobsen, H. A. (2010). Liquid entrainment-Droplet size distribution for a low surface tension mixture. *Chemical Engineering Science*, *65*(18), 5272–5284. https://doi.org/10.1016/j.ces.2010.06.038

Rodrigues, H. T., Pereyra, E., & Sarica, C. (2018). A model for the thin film friction factor in near-horizontal stratified-annular transition two-phase low liquid loading flow. *International Journal of Multiphase Flow*, *102*, 29–37. https://doi.org/10.1016/j.ijmultiphaseflow.2018.01.017

Shmueli, A., Unander, T. E., & Nydal, O. J. (2015). Characteristics of gas/Water/Viscous oil in stratified-Annular horizontal pipe flows. In *OTC Brasil 2015: The Atlantic: From East to West - An Ocean of Innovation* (pp. 1085–1102). https://doi.org/10.4043/26176-ms

Tso, C. P., & Sugawara, S. (1993). Corrective technique for numerical prediction of liquid flow rate in annular flow study. *Communications in Numerical Methods in Engineering*, *9*(6), 533–542. https://doi.org/10.1002/cnm.1640090611

van 't Westende, J. M. C., Belt, R. J., Portela, L. M., Mudde, R. F., & Oliemans, R. V. A. (2007). Effect of secondary flow on droplet distribution and deposition in horizontal annular pipe flow. *International Journal of Multiphase Flow*, *33*(1), 67–85.

https://doi.org/10.1016/j.ijmultiphaseflow.2006.07.004

Vieira, R. E., Kesana, N. R., Torres, C. F., McLaury, B. S., Shirazi, S. A., Schleicher, E., & Hampel, U. (2014). Experimental investigation of horizontal gas–liquid stratified and annular flow using wire-mesh sensor. *Journal of Fluids Engineering*, *136*(12), 121301.

Vieira, R. E., Kesana, N. R., Torres, C. F., McLaury, B. S., Shirazi, S. A., Schleicher, E., & Hampel, U. (2013). Experimental Investigation of Horizontal Gas-Liquid Stratified and Annular Flow using Wire Mesh Sensor. *Proceedings of the ASME 2013 Fluids Engineering Division Summer Meeting*, 1–8.

Wang, Y., Yu, Y., Liu, Z., Chang, Y., Zhao, X., & Wang, Q. (2024). Experimental Study on Gas-Liquid Two-Phase Stratified Flow at High Pressure in a Horizontal Pipe. *Energies*, *17*(5). https://doi.org/10.3390/en17051056

Yang, K., Liu, J., Wang, M., Wang, H., & Xiao, Q. (2023). Identifying Flow Patterns in a Narrow Channel via Feature Extraction of Conductivity Measurements with a Support Vector Machine. *Sensors*, *23*(4). https://doi.org/10.3390/s23041907

Yaws, C. L. (2015). The Yaws Handbook of Physical Properties for Hydrocarbons and Chemicals. In *Elsevier*.

Zhao, Y., Markides, C. N., Matar, O. K., & Hewitt, G. F. (2013). Disturbance wave development in two-phase gas-liquid upwards vertical annular flow. *International Journal of Multiphase Flow*, *55*, 111–129. https://doi.org/10.1016/j.ijmultiphaseflow.2013.04.001